Archives of Dermatological Research (2019) 311:317–324
https://doi.org/10.1007/s00403-019-01905-0

ORIGINAL PAPER

# Modulation of lipid fluidity likely contributes to the fructose/xylitol-induced acceleration of epidermal permeability barrier recovery

**Yuki Umino**[1,3] · **Sari Ipponjima**[2] · **Mitsuhiro Denda**[1]

Received: 5 August 2018 / Revised: 8 January 2019 / Accepted: 1 March 2019 / Published online: 7 March 2019


## Abstract

We previously showed that topical application of hexoses such as fructose accelerates barrier recovery after disruption. We also showed that various hexoses and polyols interact with phospholipid and alter the phase transition temperature. Thus, we hypothesized that the improvement of barrier recovery by hexoses and polyols might be related to the interaction with phospholipid. Here, we tested this idea by examining the effects of xylitol (a component of some skin-care products) and fructose on lipid dynamics in an epidermal-equivalent model at the single-cell level by means of two-photon microscopy after staining with Laurdan, a fluorescent dye sensitive to the physical properties of its membrane environment. First, we confirmed that topical application of xylitol aqueous solution on tape-stripped human skin accelerated barrier recovery. Then, we examined changes of lipid fluidity in the epidermal-equivalent model after application of water or an aqueous solution of xylitol or fructose. Application of xylitol and/or fructose increased the lipid fluidity in the uppermost part of the stratum granulosum layer, compared to treatment with water alone, and accelerated the exocytosis of lamellar bodies to the intercellular domain between stratum corneum and stratum granulosum. Our results support the idea that the improvement of epidermal barrier homeostasis upon topical application of xylitol or fructose is due to increased lipid fluidity in the uppermost layer of the stratum granulosum, which enables accelerated release of lipid from the stratum granulosum, thereby improving the lamellar structure and accelerating epidermal permeability barrier recovery.

**Keywords** Lipid fluidity · Epidermal permeability barrier · Stratum granulosum · Lamellar body · Two-photon microscope

## Introduction

We previously demonstrated that topical application of certain hexoses influenced the recovery rate after barrier disruption of barrier function. For example, application of mannose and fructose accelerated the barrier recovery, while galactose and glucose had no effect [1]. We also found that mannose and fructose increased the membrane pressure of phospholipid monolayer or the stability of liposomes [17]. We further reported that several polyols, including xylitol, increased the membrane pressure and altered the phase transition temperature of phospholipids. Therefore, these polyols appear to stabilize the liquid crystal phase at low temperature [15, 16].

The exocytosis of lamellar bodies in the uppermost layer of the epidermis is a crucial step for barrier recovery [10]. During this process, phase transition between lamellar bodies and the cell membrane might be induced [18]. The results of the physico-chemical studies described above suggest that molecules that accelerate the barrier recovery tend to stabilize the liquid crystalline phase, resulting in an increase in the fluidity of lipid lamellar structure in the uppermost part of the living layer of the epidermis.

In this study, we focused on xylitol and fructose, since they influence barrier function in vivo [1, 12] and alter the phase transition temperature of phospholipids [16, 17]. Thus, we evaluated the effect of application of xylitol or fructose on lipid fluidity in the epidermal-equivalent models, using a fluorescent probe, Laurdan. Our results suggest that the methodology

**Electronic supplementary material** The online version of this article (https://doi.org/10.1007/s00403-019-01905-0) contains supplementary material, which is available to authorized users.

✉ Yuki Umino
yuki.umino@to.shiseido.co.jp

[1] Shiseido Global Innovation Center, Yokohama, Japan

[2] Research Institute for Electronic Science, Hokkaido University, Sapporo, Japan

[3] Shiseido Global Innovation Center, 2-2-1, Hayabuchi, Tsuzuki-ku, Yokohama, 224-8558 Japan

described here could be a useful tool for the investigation of epidermal permeability barrier homeostasis, and for screening agents that modulate exocytosis of lamellar bodies.

## Methods

### Barrier recovery upon topical application of xylitol

Seven males in their 20s–30s were studied in an environment maintained at a temperature of 20–22 °C and a relative humidity of about 45%. Barrier function was evaluated by measurement of transepidermal water loss (TEWL) with an electrolytic moisture analyser (Meeco, Warrington, PA, USA). Skin on the inside forearm was repeatedly tape-stripped (about 30 times). Immediately thereafter, TEWL was measured and 10 µl of water and 100 mM xylitol aqueous solution were applied at different sites. The application sites were wrapped for 10 min, and then the wrapping and remaining solutions were removed. TEWL was measured at the same sites at 1.5 and 3 h after barrier disruption. In each subject, the barrier recovery rate was calculated according to the following formula: (TEWL immediately after barrier disruption – TEWL at indicated time point)/(TEWL immediately after barrier disruption – baseline TEWL) × 100%.

### Construction of the epidermal-equivalent model

The protocol for construction of the epidermal-equivalent model was described previously [13]. Normal human epidermal keratinocytes (NHEKs) from Kurabo (Osaka, Japan) were cultured in Epilife-KG2 (Kurabo) containing 0.06 mM $Ca^{2+}$. Keratinocytes ($2.2 \times 10^5$/500 µl of CnT Prime medium; CELLnTEC, Bern, Switzerland) were plated on 12-well millicells with hanging 0.4 µm PET inserts (Millipore, Billerica, MA). The inserts were precoated with CellStart (Invitrogen Life Technologies, Carlsbad, CA) in a 50× DPBS dilution. CnT Prime medium was added to the well. After 3 days, the medium was switched to CnT-PR-3D differentiation medium (CELLnTEC, Bern, Switzerland) containing 50 µg/ml vitamin C both on the inside and outside of the inserts. On the following day, cultures were lifted to the air-medium interface by removing the excess medium from the insert and reducing the volume of differentiation medium on the outside to 500 µl. Cultures were fed every day with 500 µl of differentiation medium for 8 days.

### Staining and observation

Cultures were treated with 20 µM Laurdan (Invitrogen Life Technologies, Carlsbad, CA) in CnT-PR-3D differentiation medium 2 days before observation, then treated with 20 µM Laurdan and 2 µM Cell Tracker Red CMTPX Dye (Thermo Fisher Science, Waltham, MA) in differentiation medium a day before observation. When Nile Red was used, cultures were treated with 0.05 µg/ml Nile Red (Sigma-Aldrich, St. Louis, Missouri) in the medium overnight. When polyols were applied, 200 µl of water or 100 mM polyol was added on the top of the stratum corneum and the plates were incubated at 37 °C for 2 h. Then the solution was removed and incubation was continued at 37 °C for 1 h. In case of application of acetone/ether, 200 µl of water or acetone/ether mixture was added on the top of the stratum corneum and the plates were incubated for 3 min. Then the remaining solutions after evaporation and absorption were removed. Treatment was carried out twice.

Laurdan imaging was done with a two-photon microscope at 440 nm (range from 426 to 450 nm) and 490 nm (range from 467 to 499 nm). The generalized polarization (GP) value was calculated from the following formula: $(I_{440nm} - I_{490nm}) / (I_{440nm} + I_{490nm})$. A higher GP value indicates lower fluidity of the lipids and a lower value indicates high fluidity [19]. GP values were calculated from the average values of the entire field of images (Fig. 3, S1) or from the average values of ROIs at the single-cell level in the case of the stratum granulosum (Figs. 4, 5).

### Electron-microscopic observation

Epidermal-equivalent models were fixed overnight in modified Karnovsky's fixative and post-fixed in 2% aqueous osmium tetroxide as described previously [6]. After fixation, all samples were dehydrated in graded ethanol solutions, and embedded in Epon–epoxy mixture. Thin sections were stained with lead citrate and uranyl acetate and viewed with an electron microscope.

### Statistics

The results are expressed as the mean ± SD. The statistical significance of differences between two groups was determined by applying Student's *t* test (Figs. 1, 7). In the case of three or more groups, statistical significance was determined by ANOVA with Tukey's test (Fig. 5) or Scheffé's test (Fig. 6), as implemented in KaleidaGraph (HULINKS, Tokyo, Japan).

## Results

As shown in Fig. 1, we first confirmed that topical application of xylitol aqueous solution on human skin after barrier disruption significantly accelerated the barrier recovery.

Then, to investigate the lipid fluidity of the granular cells, we used an epidermal-equivalent model. Images of cells co-stained with Laurdan and Nile Red in the uppermost

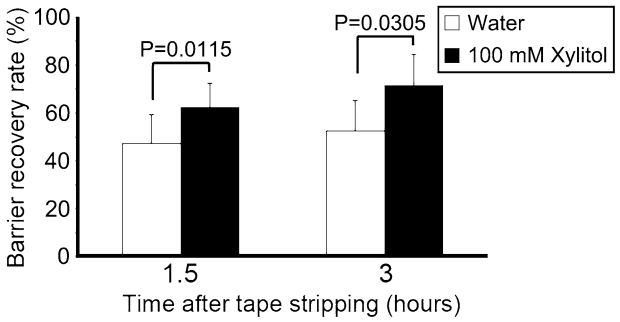


**Fig. 1** Barrier recovery rate after topical application of water or 100 mM xylitol aqueous solution. Results are mean ± SD ($n = 7$) ($p$ values were calculated by Student's $t$ test)

granular layer are shown in Fig. 2. As previously reported, intracellular lipid structure surrounding the nucleus was clearly visualized by Laurdan and Nile Red [9, 14].

A 3D image of the model stained with Laurdan and Cell Tracker red is shown in Fig. 3a. Images of each layer are shown in Fig. 3b. The border between stratum corneum and stratum granulosum was defined in terms of the presence/absence of nuclei, and appeared to lie at around 12 µm from the skin surface. A representative profile of the GP value is shown in Fig. 3c. Images surrounded by a red line in Fig. 3b correspond to the red box in Fig. 3c. In the stratum corneum, the GP value was highest in the deeper layer. In the stratum granulosum, the GP value was lowest in the upper layer at around 14 µm from the skin surface.

We next focused on single cells in each layer (Fig. 4a, b, c). A representative profile of the GP value is shown in Fig. 4d. The positions indicated with red letters in Fig. 4d (I, II, III) correspond to the locations indicated by red lines (Fig. 4e) in the upper layer of the epidermis. The GP value was lowest (GPII) at around 14–15 µm from the skin surface; i.e., the lipid fluidity is highest in this location. Comparison of Figs. 3 and 4 indicates that the GP profile in the epidermal model is consistent with the findings at the single-cell level.

Next, we stained the epidermal model with Laurdan after application of various solutions and analyzed the GP values at the single-cell level. Representative profiles of GP values of the model treated with water, xylitol aqueous solution, and fructose aqueous solution for 2 h are shown in Fig. 5a, b, c and the profiles observed after treatment with water and acetone/ether solution twice for 3 min each are shown in Fig. 5d, e. Below each profile, the average GPII value (the lowest GP value in the uppermost part of the stratum granulosum) is shown. Application of either xylitol or fructose aqueous solution significantly decreased the GPII value. In the former case (Fig. 5a, b, c), the stratum corneum became thicker (16–18 µm). We speculated that during the 2-h application of water, xylitol or fructose aqueous solution, the stratum corneum was swollen by hydration. Treatment with acetone/ether significantly increased the GPII values. These results indicate that treatment with xylitol or fructose solution increased lipid fluidity in the uppermost layer of the stratum granulosum, while acetone/ether treatment decreased it. On the other hand, we observed no change of GP value (lipid fluidity) in the lipids of the stratum corneum after treatment with xylitol or fructose or acetone/ether. Representative GP profiles in the stratum corneum are shown in figure S1. These results suggest that the application of these

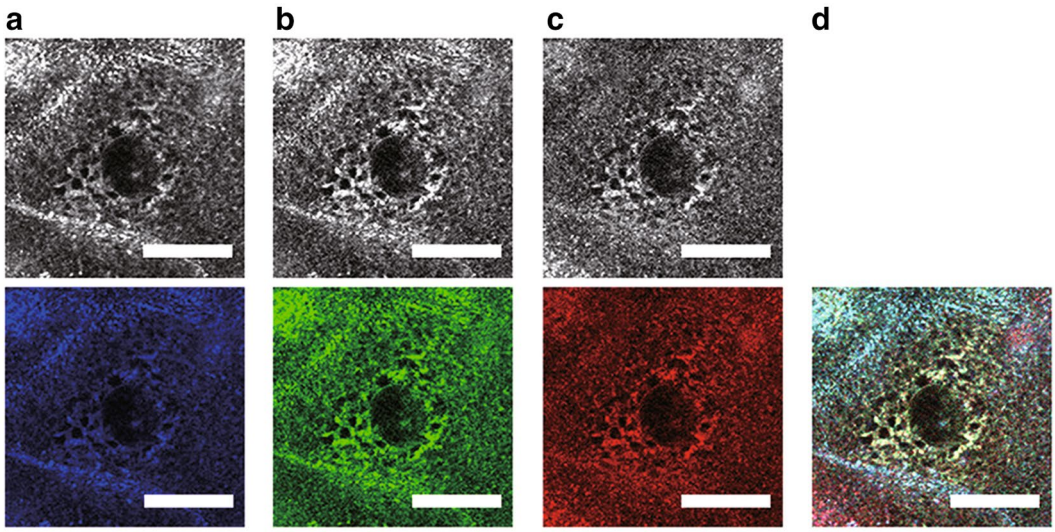


**Fig. 2** Images of cells in the uppermost layer of the epidermal granulosum stained with (**a**) Laurdan at 440 nm (blue), (**b**) Laurdan at 490 nm (green), (**c**) Nile Red (red) and (**d**) merge. Scale bar 20 µm

solutions mainly affected the lipids in the stratum granulosum, but had little effect on the lipids in the stratum corneum.

Electron-microscopic images of the uppermost layer of the epidermis after the corresponding treatment are shown (Figs. 6, 7). Treatments with xylitol or fructose solution accelerated the exocytosis of lamellar bodies to the intercellular domain between stratum corneum and stratum granulosum (Fig. 6b, c, white asterisks). On the other hand, acetone/ether treatment induced cavities in the intercellular domain between stratum corneum and stratum granulosum (Fig. 7b, black asterisks). The results of quantitative evaluation after application of xylitol or fructose (compared with water) are shown in Fig. 6d, and those after acetone/ether treatment (compared with water) are shown in Fig. 7c. These results indicate that intercellular lipid domains were significantly increased after application of xylitol and fructose, and significantly decreased after treatment of acetone/ether. These electron microscopy findings correspond well to the lipid fluidity observations.

**Fig. 4** Single-cell level images at each layer of the epidermal model. ▶ Images of each layer in the epidermal-equivalent model at the single-cell level in the uppermost stratum granulosum layer stained with **a** Laurdan (440 nm: blue, 490 nm: green) and Cell Tracker red (red), **b** Laurdan at 440 nm and **c** Laurdan at 490 nm. *Z* step = 0.65 µm. White numbers at the bottom left indicated the depth from the skin surface (µm). Scale bar 20 µm. **d** Representative profile of the GP values. *Z* step = 0.325 µm. **e** Schematic illustration of the locations of the three points marked in (**d**): I is the lowermost stratum corneum, II is the center of the uppermost part of the stratum granulosum and III is the boundary between the uppermost stratum granulosum and the next lower layer. Average GPII value (the GP value at the center of the uppermost stratum granulosum) is mean ± SD ($n = 15$)

## Discussion

In moving towards the skin surface, the GP value reached a minimum in the uppermost living layer (stratum granulosum) of the untreated epidermal-equivalent model, then increased in the deeper part of the stratum corneum and finally decreased sharply at the upper layer of the stratum corneum. This seems reasonable, because the barrier function is highest at the deeper layer of the stratum corneum and becomes lower at the upper layer [11].

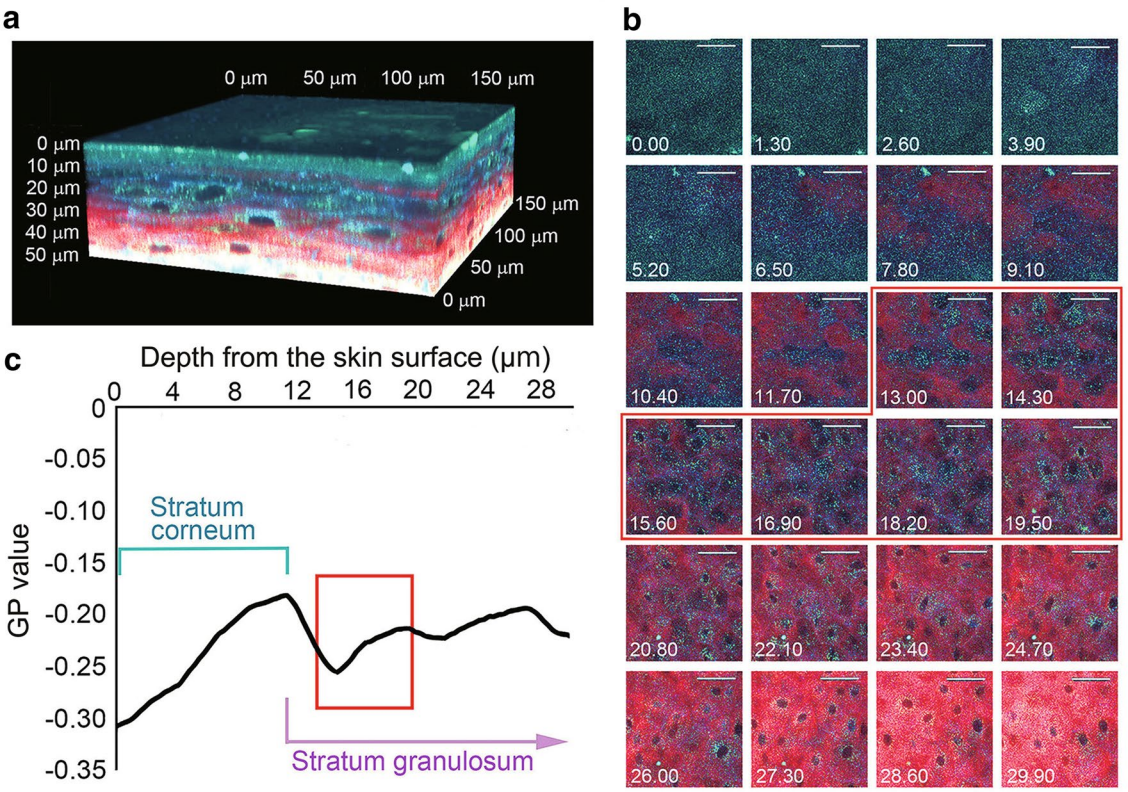


**Fig. 3** 3D image of the epidermal model stained with Laurdan and Cell Tracker red. **a** 3D image and **b** images of each layer in the epidermal-equivalent model stained with Laurdan (440 nm: blue, 490 nm: green) and Cell Tracker red (red). *Z* step = 0.325 µm or 1.3 µm. White numbers at the bottom left indicated the depth from the skin surface (µm). Scale bar 50 µm. **c** Representative profile of the GP value. *Z* step = 0.325 µm. Images surrounded by the red line in Fig. 3b correspond to the red box in Fig. 3c

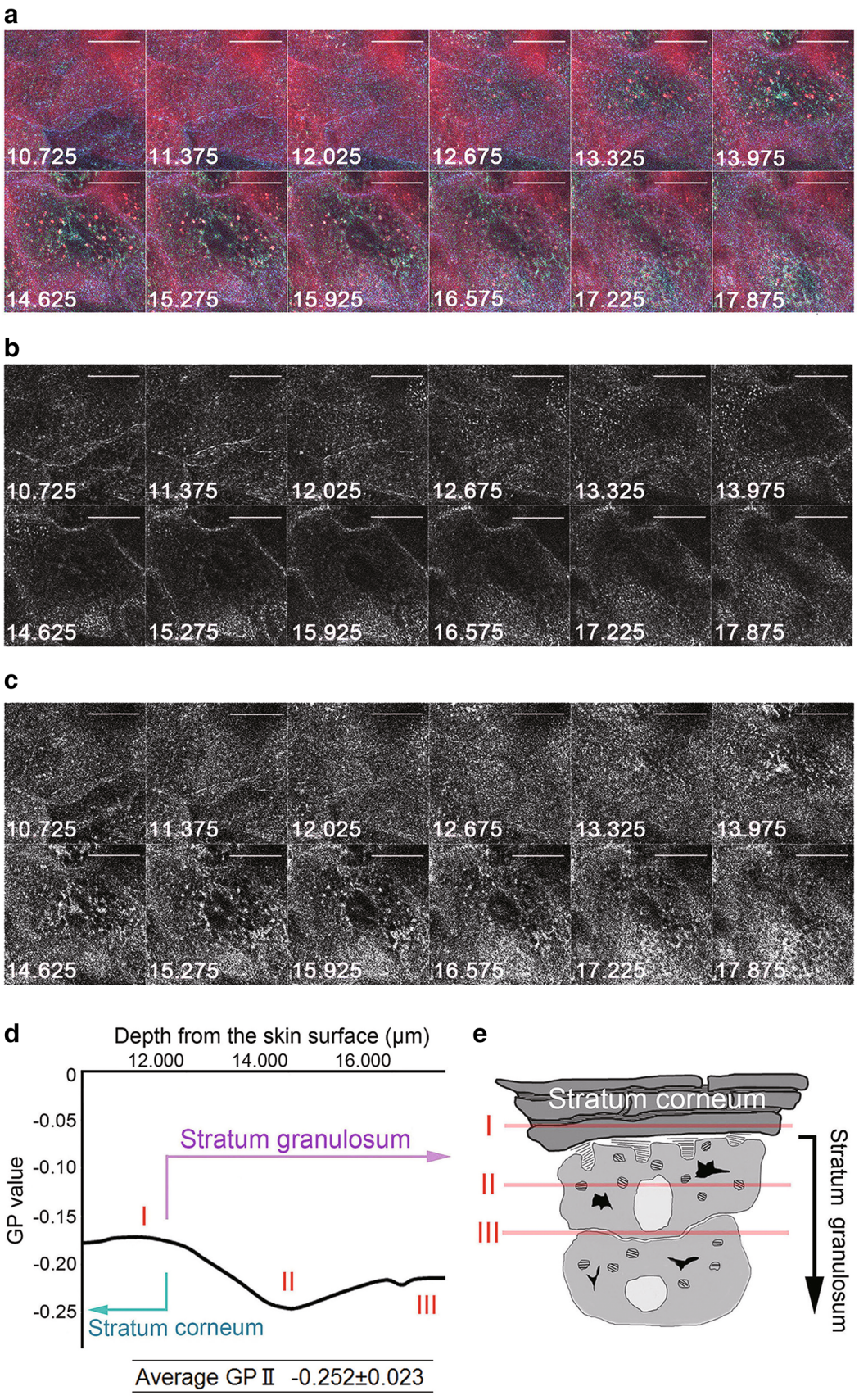
a
10.725
11.375
12.025
12.675
13.325
13.975
14.625
15.275
15.925
16.575
17.225
17.875
b
10.725
11.375
12.025
12.675
13.325
13.975
14.625
15.275
15.925
16.575
17.225
17.875
c
10.725
11.375
12.025
12.675
13.325
13.975
14.625
15.275
15.925
16.575
17.225
17.875
d
Depth from the skin surface (μm)
12.000
14.000
16.000
0
-0.05
-0.10
-0.15
-0.20
-0.25
GP value
Stratum granulosum
I
II
III
Stratum corneum
Average GP Ⅱ -0.252±0.023
e
Stratum corneum
I
II
III
Stratum granulosum

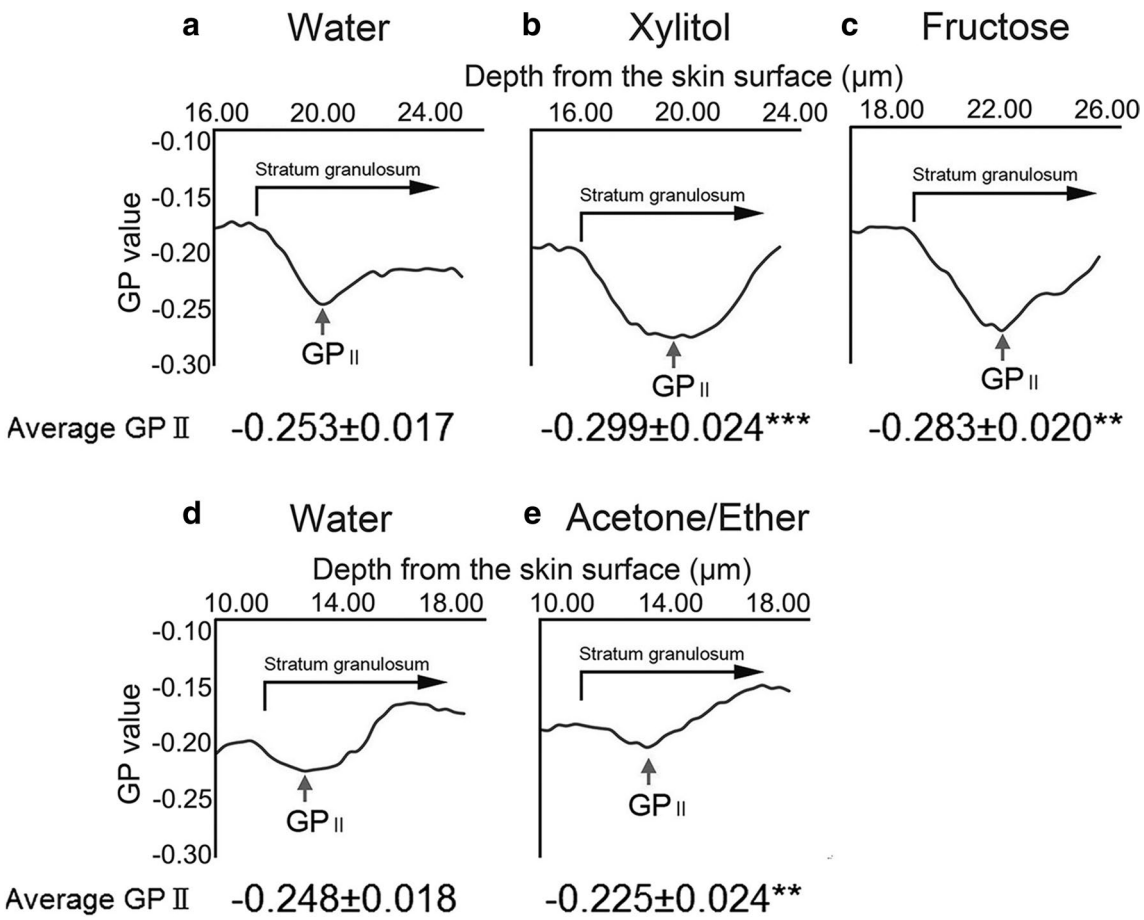


**Fig. 5** Representative profiles of GP value at the single-cell level in the uppermost part of the stratum granulosum and average GPII values after application of **a** water, **b** xylitol, **c** fructose **d** water (control of acetone/ether) and **e** acetone/ether. Arrows indicate the GPII value (the GP value at the center of the uppermost part of the stratum granulosum). Below each profile, the average GPII values is shown: mean ± SD ($n = 15$). $^{**}p < 0.01$ and $^{***}p < 0.001$ versus the untreated model (Fig. 4) or application of water (Fig. 5a, d). ($p$ values were calculated by ANOVA with Tukey's test). Similar results were obtained in four independent experiments

Tightly organized intercellular lipid structure is necessary for barrier function [5]. Thus, at the deeper layer of the stratum corneum, intercellular lipid molecules might be tightly organized, and the lipid fluidity might be lower. At the upper layer of the stratum corneum, because of the degradation of desmosomes, the lipid lamellar structure becomes looser [20]. This is in accordance with the finding that the GP value decreases at the uppermost part of the stratum corneum in the epidermal-equivalent model.

Previous studies have demonstrated that in the uppermost layer of the epidermal living layer (stratum granulosum), lamellar bodies are fused to each other, forming a network structure [7, 9]. Here, we directly observed the intercellular lipid in the uppermost layer of the epidermal living layer (Fig. 2). It is reported that exocytosis of lamellar bodies occurs into the intercellular domain between stratum granulosum and stratum corneum [18]. In this study, the GP value became lower after application of xylitol or fructose, indicating that the lipid fluidity is increased. Thus, lipid fluidity might be an important factor for exocytosis of lamellar bodies.

Clearly, the in vitro system used in the present study is different from in vivo skin; for example, its water-impermeable barrier function is lower than that of intact skin (data not shown). However, exocytosis of lamellar bodies is a critical step in barrier recovery [18]. Here, we observed the exocytosis of lamellar bodies to the intercellular domain between stratum corneum and stratum granulosum by electron microscopy in our model (Fig. 6). Further, these observations correspond well to the changes in lipid fluidity (Fig. 5a, b, c). Thus, although this in vitro system may not fully reflect the in vivo barrier, we considered that it is useful to evaluate exocytosis of lamellar bodies.

We previously demonstrated that the topical application of fructose after barrier disruption accelerated barrier recovery [1]. Here, we demonstrated that the application of

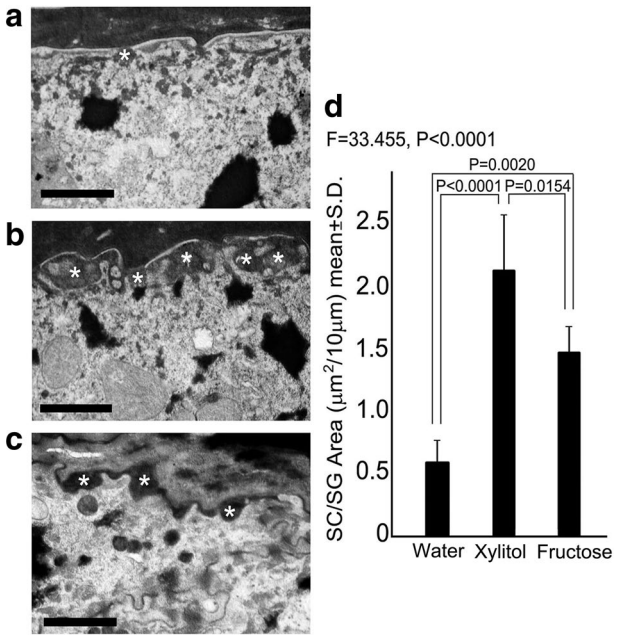


**Fig. 6** Representative electron-microscopic images showing the uppermost layer of the epidermis after application of **a** water, **b** xylitol, or **c** fructose. White asterisks indicate exocytosis of lamellar bodies in the intercellular domain between stratum corneum and stratum granulosum (**a**–**c**). Scale bar 1 μm. **d** Results of quantitative evaluation of stratum corneum/stratum granulosum (SC/SG) lipid domains (*p* values were calculated by ANOVA with Scheffé's test)

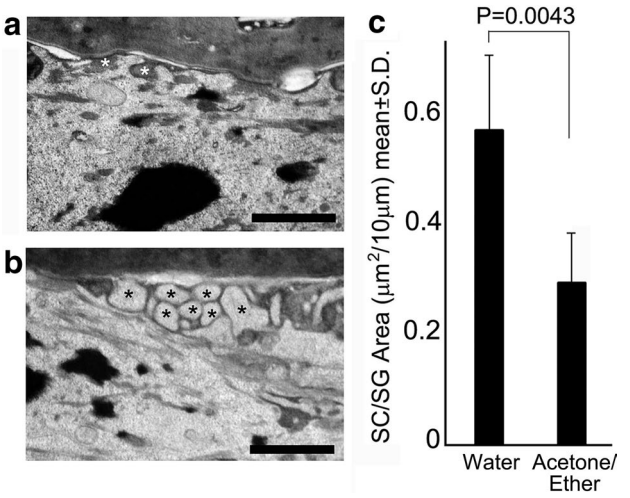


**Fig. 7** Representative electron-microscopic images showing the uppermost layer of the epidermis after application of (**a**) water (control) and (**b**) acetone/ether. White asterisks indicate exocytosis of lamellar bodies in the intercellular domain between stratum corneum and stratum granulosum (**a**) and black asterisks indicate cavities in the intercellular domain between stratum corneum and stratum granulosum (**b**). Scale bar 1 μm. (**f**) Results of quantitative evaluation of stratum corneum/stratum granulosum (SC/SG) lipid domains (*p* values were calculated by Student's *t* test)

xylitol also accelerated barrier recovery (Fig. 1). Thus, both fructose and xylitol, which interact with phospholipids [16, 17], appear to increase lipid fluidity in the uppermost living layer of the epidermal-equivalent model, compared to water and promote exocytosis of lamellar bodies in the uppermost layer of the epidermis, thereby accelerating barrier recovery.

In the present study, acetone/ether treatment decreased the fluidity of the lipid phase, and we observed cavities between the stratum corneum and stratum granulosum by electronic microscopy (Fig. 7b). The acetone/ether treatment presumably disrupted lipids, and might have affected the epidermal viability. We cannot rule out the possibility that lipids in the stratum granulosum were at least partly extracted by acetone/ether. However, there was no significant change of GP profile in the stratum corneum (figure S1b). Previous studies have demonstrated that barrier disruption by tape stripping or acetone treatment accelerates secretion of lamellar bodies to the intercellular domain between stratum granulosum and stratum corneum, initiating recovery of the barrier function, and then lipid synthesis starts to supplement this process [8]. In other words, restoration of the network structure between stratum granulosum and stratum corneum appears to be crucial for barrier recovery after its disruption.

Although tape stripping and acetone treatment are of course different, reagents or factors that influence barrier recovery rate appear to have similar effects after barrier disruption using either method [2–4]. We selected tape stripping for in vivo studies, because disruption of the human barrier by acetone treatment takes a long time and we wished to avoid a substantial time lag in the measurements. On the other hand, the epidermal-equivalent model is more fragile and tape stripping to disrupt the barrier is difficult to apply consistently. Thus, the results of our in vivo and epidermal-equivalent model studies are not directly comparable. However, reagents that accelerate recovery from barrier disruption by tape stripping or acetone treatment also accelerate lamellar body secretion between stratum corneum and stratum granulosum [2, 3]. Therefore, we consider that our in vitro system could be useful as a screening system for agents that modulate exocytosis of lamellar bodies.

Our previous and present findings indicate that the topical application of molecules that increase the fluidity of the lipid phase might accelerate the early stage of barrier recovery. The present approach could be useful to find molecules that improve barrier homeostasis.

**Acknowledgements** We appreciate the feedback offered by Dr. Makiko Goto (Shiseido Global Innovation Center). This work was supported by JST CREST Grant Number JPMJCR15D2, Japan.

## Compliance with ethical standards

**Conflict of interest** The authors declare that they have no conflict of interest.

**Research involving human participants and/or animals** The protocol was approved by the ethics committees of Shiseido Research Center, and was in accordance with the National Institute of Health guideline and Declaration of Helsinki principles.

**Informed consent** Informed consent was obtained from all individual participants.

## References


1. Denda M (2011) Effects of topical application of aqueous solutions of hexoses on epidermal permeability barrier recovery rate after barrier disruption. Exp Dermatol 20:943–944
2. Denda M, Fuziwara S, Inoue K (2003) Influx of calcium and chloride ions into epidermal keratinocytes regulates exocytosis of epidermal lamellar bodies and skin permeability barrier homeostasis. J Invest Dermatol 121:362–367
3. Denda M, Fuziwara S, Inoue K (2004) Association of cyclic adenosine monophosphate with permeability barrier homeostasis of murine skin. J Invest Dermatol 122:140–146
4. Denda M, Kitamura K, Elias PM, Feingold KR (1997) Trans-4-(Aminomethyl)cyclohexane carboxylic acid (T-AMCHA), an anti-fibrinolytic agent, accelerates barrier recovery and prevents the epidermal hyperplasia induced by epidermal injury in hairless mice and humans. J Invest Dermatol 109:84–90
5. Denda M, Koyama J, Namba R, Horii I (1994) Stratum corneum lipid morphology and transepidermal water loss in normal skin and surfactant-induced scaly skin. Arch Dermatol Res 286:41–46
6. Denda M, Sato J, Masuda Y, Tsuchiya T, Koyama J, Kuramoto M, Elias PM, Feingold KR (1998) Exposure to a dry environment enhances epidermal permeability barrier function. J Invest Dermatol 111:858–863
7. den Hollander L, Han H, de Winter M, Svensson L, Masich S, Daneholt B, Norlén L (2016) Skin lamellar bodies are not discrete vesicles but part of a tubuloreticular network. Acta Derm Venereol 96:303–308
8. Elias PM (2006) The epidermal permeability barrier from Saran Wrap to biosensor. In: Skin B, Elias PM, Feingold KR (eds), 2. Taylor & Francis, New York, pp 25–31
9. Elias PM, Cullander C, Mauro T, Rassner U, Kömüves L, Brown BE, Menon GK (1998) The secretory granular cell: the outermost granular cell as a specialized secretory cell. J Investig Dermatol Symp Proc 3:87–100
10. Feingold KR, Elias PM (2014) Role of lipids in the formation and maintenance of the cutaneous permeability barrier. Biochim Biophys Acta 1841:280–294
11. Kalia YN, Pirot F, Guy RH (1996) Homogeneous transport in a heterogeneous membrane: water diffusion across human stratum corneum in vivo. Biophys J 71:2692–2700
12. Korponyai C, Szél E, Behány Z, Varga E, Mohos G, Dura Á, Dikstein S, Kemény L, Erős G (2017) Effects of locally applied glycerol and xylitol on the hydration, barrier function and morphological parameters of the skin. Acta Derm Venereol 97:182–187
13. Kumamoto J, Nakanishi S, Umino Y, Denda M (2018) Removal of nontoxic foreign material to the surface by cultured human epidermal keratinocytes in an epidermal-equivalent model. J Dermatol Sci 89:97–99
14. Mazeres S, Fereidouni F, Joly E (2017) Using spectral decomposition of the signals from laurdan-derived probes to evaluate the physical state of membranes in live cells. F1000 Res 6:763
15. Nakata S, Deguchi A, Seki Y, Furuta M, Fukuhara K, Nishihara S, Inoue K, Kumazawa N, Mashiko S, Fujihira S, Goto M, Denda M (2015) Characteristic responses of a phospholipid molecular layer to polyols. Colloid Surf B Biointerfaces 136:594–599
16. Nakata S, Nomura M, Yamaguchi Y, Hishida M, Kitahata H, Katsumoto Y, Denda M, Kumazawa N (2019) Characteristic responses of a 1,2-dipalmitoleoyl-sn-glycero-3- phosphoethanolamine molecular layer depending on the number of CH(OH) groups in polyols. Colloids Surf A Physicochem Eng Asp 560:149–153
17. Nakata S, Shiota T, Kumazawa N, Denda M (2012) Interaction between a monosaccharide and a phospholipid molecular layer. Colloids Surf A 405:14–18
18. Norlén L (2001) Skin barrier formation: the membrane folding model. J Invest Dermatol 117:823–829
19. Sanchez SA, Tricerri MA, Gratton E (2012) Laurdan generalized polarization fluctuations measures membrane packing microheterogeneity in vivo. Proc Natl Acad Sci USA 109:7314–7319
20. Sato J, Denda M, Nakanishi J, Koyama J (1998) Dry condition affects desquamation of stratum corneum in vivo. J Dermatol Sci 18:163–169